

SARS-CoV-2 diagnostic testing rates determine the sensitivity of genomic surveillance programs

Received: 7 July 2022

Accepted: 11 November 2022

Published online: 9 January 2023

 Check for updates

Alvin X. Han¹✉, Amy Toporowski², Jilian A. Sacks³, Mark D. Perkins³, Sylvie Briand³, Maria van Kerkhove³, Emma Hannay², Sergio Carmona², Bill Rodriguez², Edyth Parker⁴, Brooke E. Nichols^{1,2,5,6} & Colin A. Russell^{1,5,6}✉

The first step in SARS-CoV-2 genomic surveillance is testing to identify people who are infected. However, global testing rates are falling as we emerge from the acute health emergency and remain low in many low- and middle-income countries (mean = 27 tests per 100,000 people per day). We simulated COVID-19 epidemics in a prototypical low- and middle-income country to investigate how testing rates, sampling strategies and sequencing proportions jointly impact surveillance outcomes, and showed that low testing rates and spatiotemporal biases delay time to detection of new variants by weeks to months and can lead to unreliable estimates of variant prevalence, even when the proportion of samples sequenced is increased. Accordingly, investments in wider access to diagnostics to support testing rates of approximately 100 tests per 100,000 people per day could enable more timely detection of new variants and reliable estimates of variant prevalence. The performance of global SARS-CoV-2 genomic surveillance programs is fundamentally limited by access to diagnostic testing.

Since the start of the COVID-19 pandemic in 2019, unprecedented expansion of genomic surveillance efforts has led to the generation of more than 10 million SARS-CoV-2 sequences deposited in the publicly accessible Global Initiative on Sharing Avian Influenza Data database (<https://www.gisaid.org/>) as of May 2022. These efforts have been integral to understanding the COVID-19 pandemic¹, including the identification of the Alpha variant in the United Kingdom during the fall of 2020², the Delta variant in India in late 2020³ and the Omicron variant in southern Africa in November 2021⁴. Despite the value of these efforts for monitoring the evolution of SARS-CoV-2, the intensity of genomic surveillance is highly heterogeneous across countries. High-income countries (HICs), on average, produced 16 times more

SARS-CoV-2 sequences per reported case than low- and middle-income countries (LMICs) as a result of long-standing socioeconomic inequalities and consequent underfunding of laboratory and surveillance infrastructures in LMICs⁵. To strengthen global pandemic preparedness, initiatives such as the Access to COVID-19 Tools Accelerator Global Risk Monitoring Framework, the Pan American Health Organization COVID-19 Genomic Surveillance Regional Network, the Africa Pathogen Genomics Initiative and the Global Influenza Surveillance and Response System, among others, have supported LMICs in developing pathogen genomic surveillance programs.

Because resources are finite, it is critical that sequencing sample sizes, and the diagnostic testing needed to obtain samples for

¹Department of Medical Microbiology and Infection Prevention, Amsterdam University Medical Center, University of Amsterdam, Amsterdam, the Netherlands. ²Foundation for Innovative New Diagnostics (FINN), Geneva, Switzerland. ³Department of Epidemic and Pandemic Preparedness and Prevention, Emergency Preparedness Programme, World Health Organization, Geneva, Switzerland. ⁴Department of Immunology and Microbiology, The Scripps Research Institute, La Jolla, CA, USA. ⁵Department of Global Health, School of Public Health, Boston University, Boston, MA, USA. ⁶These authors contributed equally: Brooke E. Nichols, Colin A. Russell. ✉e-mail: x.han@amsterdamumc.nl; c.a.russell@amsterdamumc.nl

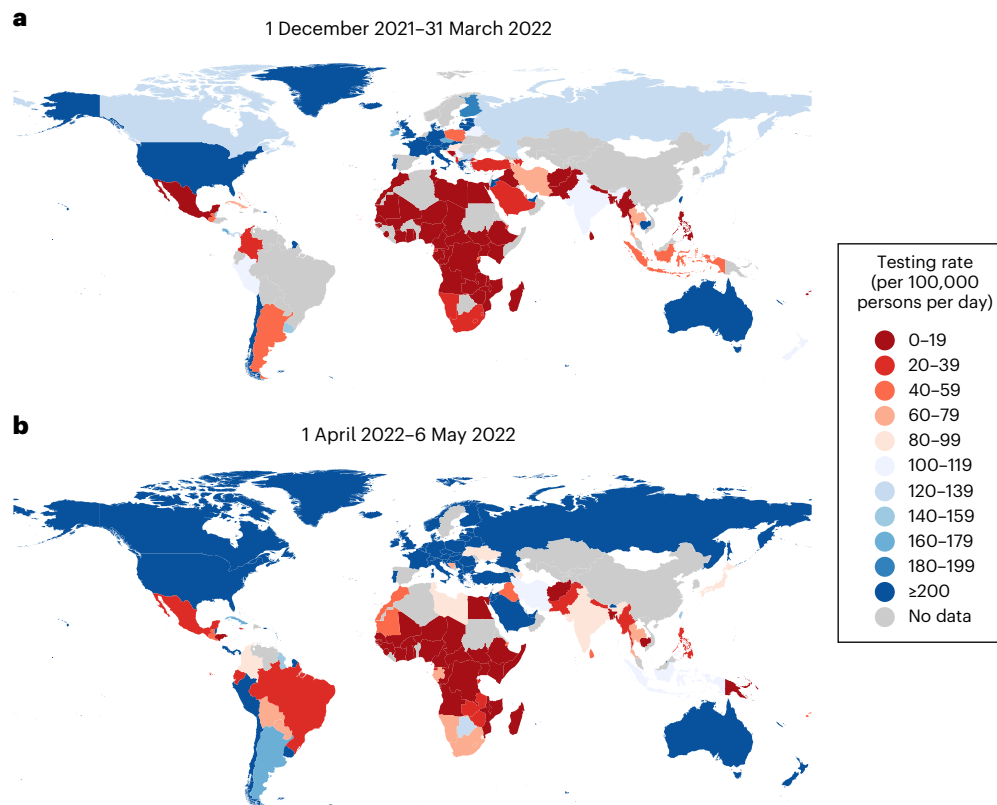


Fig. 1 | Global disparities in SARS-CoV-2 testing rates. a, b, The color of each country represents the average total number of SARS-CoV-2 tests performed per 100,000 persons per day between 1 December 2021 and 31 March 2022 when

the Omicron VOC spread around the world (a), and between 1 April 2022 and 6 May 2022 when most countries were past peak Omicron wave of infections (b)⁹. Raster map from naturalearthdata.com.

sequencing, are carefully set for genomic surveillance programs to detect and monitor variants as efficiently as possible. Current recommended sample sizes are based on sampling theory^{5–8} and assume that the volume of diagnostic testing is large enough such that the diversity of sampled viruses is representative of the diversity of viruses circulating in the population. However, LMICs test at a mean rate of 27 tests per 100,000 persons per day, as opposed to more than 800 tests per 100,000 people per day across HICs, based on observational data collected between January 2020 and March 2022⁹, with even higher testing rates in some HICs (Fig. 1). Low testing rates lead to spotty information and smaller virus specimen pools available for sequencing, resulting in sampling biases. These factors can render efforts to monitor the emergence of new SARS-CoV-2 variants or prevalence of existing variants highly unreliable.

Here, we studied how different testing rates can impact genomic surveillance outcomes. Specifically, we developed and used the Propelling Action for Testing And Treating (PATAT) model, an individual-based modeling framework, to simulate concurrently circulating wild-type SARS-CoV-2 (pre-Alpha viruses)/Alpha-like epidemics and Delta/Omicron (BA.1)-like epidemics in Zambia as a representative LMIC archetype where recent demographic census data required by the model was available (Methods). We assumed that Alpha and Omicron (BA.1) were more transmissible than the respective extant virus to achieve growth rates of approximately 0.15 and 0.35 per day, respectively^{2,10}, and simulated SARS-CoV-2 infection waves in a population of 1,000,000 individuals over a 90-day period that begins with an initial 1% prevalence of the extant SARS-CoV-2 variant and the mutant variant being introduced at 0.01%. We assumed that clinic-based, professional-use antigen rapid diagnostic tests (Ag-RDTs) form the basis of testing, given persistent reports that polymerase chain reaction

(PCR) tests are poorly accessible for detection of individuals with COVID-19 symptoms outside of tertiary medical facilities (for example, inpatient hospitals with personnel and facilities for advanced medical investigation and treatment) in many LMICs¹¹.

We then simulated different genomic surveillance sampling strategies to elucidate how testing, sequencing volumes and the degree of sampling bias arising from sources of specimens jointly impact the timeliness of variant detection and the accuracy of variant monitoring (Methods). These strategies include: (1) sending all samples from community clinics and tertiary hospitals to a centralized facility for possible sequencing (that is, population-wide strategy); (2) sampling and sequencing a portion of positive specimens collected at one tertiary sentinel facility for the population of 1,000,000 simulated people (including individuals with mild symptoms seeking symptomatic testing and individuals with severe symptoms who sought tertiary care at the facility); or sampling and sequencing a portion of positive specimens collected at (3) 10%, (4) 25%, (5) 50% and (6) 100% of all tertiary sentinel facilities.

Results

Performance of current guidance

We first assessed various suggested sample sizes of positive specimens to sequence for detection of SARS-CoV-2 variants at low prevalence for simulated wild-type/Alpha and Delta/Omicron epidemics in Zambia with a mean testing rate of 27 tests per 100,000 people per day (based on the observed mean rate of testing in LMICs) (Fig. 2). We used recommended sample sizes from three prominent guidances: (1) The World Health Organization and European Centre for Disease Prevention and Control computed sample size using the binomial method^{7,8}; (2) by subsampling genomic surveillance data generated in Denmark in

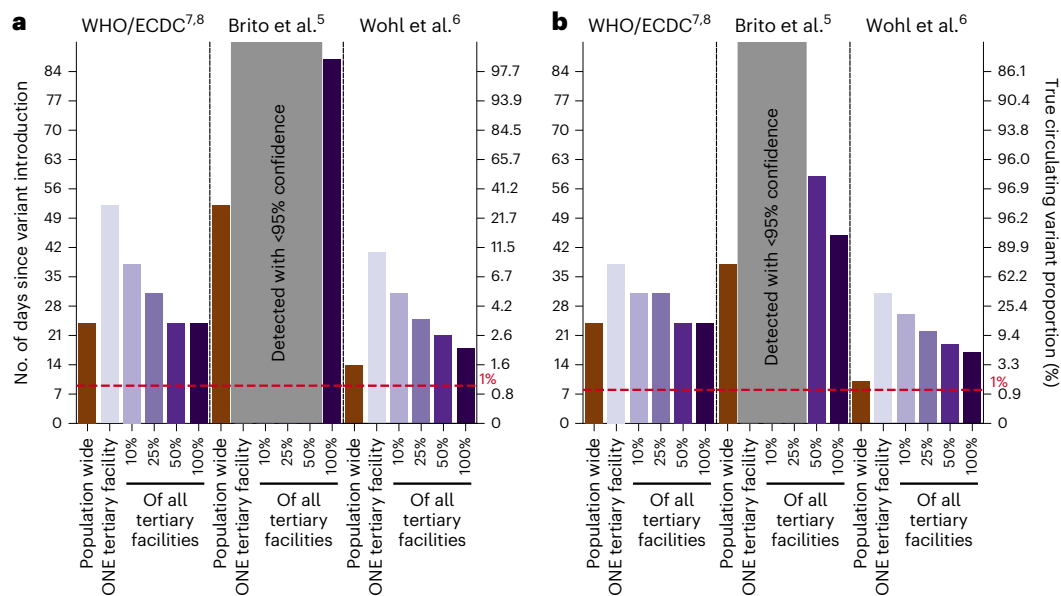


Fig. 2 | Performance of current guidance on number of positive specimens to sequence for variant detection with testing rate at 27 tests per 100,000 persons per day. First day of detection since variant introduction at 95% confidence and the corresponding circulating variant proportion using guidance from the World Health Organization (WHO)/European Centre for Disease Prevention and Control (ECDC)^{7,8}, Brito et al.⁵ and Wohl et al.⁶ (Table 1) under different genomic surveillance strategies with varying sampling coverage (that is, all collected specimens from all healthcare facilities are sent to one facility to be sampled for sequencing (population-wide strategy); or only one tertiary facility

or 10, 25, 50 or 100% of tertiary sentinel facilities would sample the specimens they collected for sequencing). Turnaround time (that is, time from specimen collection to acquisition of sequencing data) was assumed to be negligible. We performed 1,000 random independent simulations for each guidance/surveillance strategy. **a, b**, We simulated epidemics for wild-type SARS-CoV-2/Alpha (**a**) and Delta/Omicron (**b**). Gray regions denote that we could not reliably detect the variant virus with 95% confidence using the guidance in question under the assumed genomic surveillance strategy.

2020–2021 when the country was testing at more than 2,000 tests per 100,000 people per day on average, Brito et al.⁵ suggested that sequencing 0.5% of all detected cases, with a turnaround time of 21 days, would result in 20% variant detection before reaching 100 cases; and (3) Wohl et al.⁶ formulated a mathematical framework computing sequencing sample size by modeling the biological and logistical processes that impact sampled variant proportions. Critically, all three methods did not consider how low testing rates and spatial nonuniformity in sampling coverage impact sampled variant proportions and, in turn, speed of variant detection. The assumptions, mathematical background and lack of accounting for spatiotemporal bias in sample size estimation of each guidance are detailed in Table 1 and Supplementary Notes (see ‘Background on current guidance’ in Supplementary Notes).

As such, even when assuming negligible turnaround time (that is, time from specimen collection to acquisition of sequencing data), the recommended approaches were insufficient to detect the variant at their respective detection targets (for example, at 1% variant proportion or before 100 detected variant cases) when testing rates were low due to poor representativeness, regardless of the genomic surveillance sampling strategy. The first strategy of sampling specimens collected from the whole population that were sent to one sequencing facility (that is, population-wide strategy) led to the best performance (closest to detection target) for all recommendations because it involves random uniform sampling of all available samples, a fundamental assumption made by all current guidance. However, if the specimen pools available for sequencing are restricted to those collected from a subset of sentinel tertiary facilities only, the nonuniformity in sampling coverage results in spatiotemporal bias within the sequenced samples and leads to delayed detection of variants of concern (VOCs), which gets progressively worse as the proportion of tertiary facilities performing sequencing decreases to one facility.

Variant detection

To elucidate how SARS-CoV-2 testing rates and the proportion of positive specimens sequenced impact the speed of variant detection, we simulated wild-type SARS-CoV-2/Alpha and Delta/Omicron epidemics at different Ag-RDT availability, ranging from 27 to 1,000 tests per 100,000 persons per day (Fig. 3). We assumed that specimens to be sequenced are sampled on their collection day, and varied the proportion of positive specimens to sample for sequencing each day between 1 and 100%. We analyzed the impact of testing rates and sequencing proportions on the expected day when the first specimen sampled for sequencing containing the variant was collected as a measure of variant detection speed. In Fig. 3, we did not consider the time between sample collection and sequencing nor the turnaround time to obtaining sequencing results as they would only delay the actual day of variant detection by the assumed turnaround time.

For all testing rates, the relationship between the expected day when the first sample containing the variant was collected and the proportion of positive specimens sequenced per day can be described by a convex operating curve, reflecting rapidly diminishing returns in the speed of variant detection as more specimens are sampled for sequencing. Across all genomic surveillance sampling strategies, relatively larger marginal improvements to the speed of variant detection are generally made when the sequencing proportion is increased up to approximately 10% of all samples collected. Further sequencing only minimally shortens the expected time to variant detection, as the operating curve asymptotically approaches the earliest possible day of detection. Importantly, increasing SARS-CoV-2 testing allows smaller sequencing proportions to attain similar detection day targets, and higher testing rates lower the earliest possible detection day. For both the Alpha and Omicron variants, increasing testing rates from 27 to 100 tests per 100,000 persons per day brings forward the expected day of sampling the first variant sequence by at least 1 week (Fig. 3).

Table 1 | Current guidance by various stakeholder and academic groups on the number of specimens to sequence for detection of novel variants at low prevalence

	Recommendation on number/proportion of positive specimens to sequence	Critical considerations
World Health Organization/European Centre for Disease Prevention and Control ^{7,8}	Minimum number of sequences to detect at 1% variant proportion with 95% confidence for given number of reported cases: <ul style="list-style-type: none"> • 141 (<1,000 cases) • 196 (1,001–2,500 cases) • 243 (2,500–5,000 cases) • 270 (5,001–10,000 cases) • 285 (>10,000 cases) 	<ul style="list-style-type: none"> • Agnostic to variant properties • Assumes specimen pool to be sampled for sequencing is representative of circulating diversity but acknowledges that, unless testing coverage is evenly distributed, this will be a biased sample • Notes that, in countries with limited sequencing capacity, monitoring relative prevalence of variants should be prioritized
Brito et al. ⁵	At least 0.5% of all cases, with a turnaround time of 21 days to detect novel lineage before it reaches 100 cases at 20% probability	Based on sequencing data from Denmark, which is testing at an average of >2,000 tests per 100,000 persons per day ⁹
Wohl et al. ⁶	1–29 sequences per day to detect an Alpha-like variant based on 0.03% initial introduction for a population of 10,000 (assuming growth rate of 0.1 per day) at 1% variant proportion with 95% confidence ⁹	<ul style="list-style-type: none"> • Assumes that the observed variant proportion in the positive specimens collected is representative of the circulating variant proportions among the infected population. This requires a large number of specimens that are randomly collected for assumption to hold true at low circulating variant proportions • A correction factor is included to correct for biases in the observed variant proportion, but only pertaining to those arising from the relative differences in diagnostic sensitivity, sample qualities and conditional asymptomatic and symptomatic testing probabilities between the two circulating variants

⁹We used the spreadsheet (<https://github.com/HopkinsIDD/VOCsamplesize>) provided and input appropriate parameters to obtain the recommendation relevant to the simulated epidemics.

For the same level of testing and sequencing proportion, the population-wide strategy led to the earliest initial detection of a variant sequence. If sequencing were restricted to samples collected at a subset of tertiary sentinel facilities only, increasing the number of facilities sending samples for sequencing reduced the spatiotemporal bias in the specimen pool, thereby shaping the operating curves closer to the ones observed for the population-wide strategy. Interestingly, results similar to the population-wide strategy could be attained if all tertiary facilities acted as sentinel sites and sent the samples they collected for sequencing to increase the representativeness of sampling.

Observed variant proportion

Test availability and sampling coverage also affect the accuracy of the observed variant proportion (Fig. 4 and Extended Data Fig. 1). At a testing rate of 27 tests per 100,000 persons per day, the observed variant proportion maximally differs from the true circulating proportion by more than 30% of the true value for both the Alpha and Omicron variants and, for more than 15% of the time, the proportional difference between the observed and true variation was greater than 20%. Both the maximum absolute difference and percentage of time points where the difference is greater than 20% can be lowered to less than 20% and less than 5%, respectively, if the testing rate is increased to 100 or more tests per 100,000 people per day.

Critically, when the representativeness of the specimen pool is spatiotemporally biased by sequencing samples collected at tertiary sentinel facilities only, increasing the proportion of specimens to be sequenced only marginally lowers the maximum absolute difference or lessens the number of times where observed variant proportion deviates less than 20% from true circulating proportions (Fig. 4, near vertical isoclines at low daily rates of testing). Increasing testing rates at sentinel surveillance sites provides more accurate detection in changes to circulating prevalence than sequencing more samples in the context of low testing rates.

Sensitivity analyses

We repeated our analyses using virus properties (that is, incubation period, maximum viral load, protection against infection by the mutant virus after extant virus infection) of the Omicron variant, but varied different relative transmissibility to the Delta variant (1.0 to 4.0) and the initial proportion of individuals who had been infected by the Delta variant (10 and 40%). The variant growth rates

simulated for these hypothetical Delta/Omicron epidemics ranged from 0.17 to 0.42 per day.

Under these varied conditions, the expected day when the specimen of the first variant sequence is collected still follows a convex-shaped operating curve against the daily proportion of positive specimens to sequence. For all curves, the larger marginal improvements in shortening variant detection are still in sequencing proportions of up to approximately 10% (Extended Data Fig. 2). In terms of the accuracy of observed variant to true circulating proportions, the maximum absolute difference and percentage of time points where the difference is greater than 20% are both substantially lowered if the testing rate is increased to at least 100 tests per 100,000 people per day (Extended Data Figs. 3 and 4).

We also varied the prevalence of extant Delta infections when the Omicron variant was introduced (Extended Data Fig. 5). We found that lower test availability causes a delay in sampling the first variant specimen if the variant is introduced when pre-existing extant variant circulation is high. At 27 tests per 100,000 persons per day, regardless of specimen proportions sequenced, detection could be delayed by approximately 1 week if Omicron was introduced when Delta was circulating at 10% prevalence as opposed to 1%. This is because a greater share of tests would be used to diagnose the more prevalent extant virus infections which, in turn, decreases the likelihood of detecting the newly introduced variant at low proportions.

Discussion

Our findings show that the emphasis on the proportion of samples referred for genomic surveillance is misplaced if testing capacity is insufficient and sample sources are highly spatiotemporally biased. As such, at the current mean rate of testing in LMICs (27 tests per 100,000 persons per day), current guidance^{5–8} on sequencing sample size estimation could likely lead to later-than-predicted detection of novel variants at best or, at worst, leave new variants undetected until they have infected a majority of a population.

Based on our work, we identified three major areas of improvement that could be prioritized to enhance the robustness of genomic surveillance programs (Fig. 5). First, the most substantial improvements are likely to come from increasing the mean testing rate in LMICs from 27 tests per 100,000 persons per day (Fig. 5a) to at least 100 tests per 100,000 persons per day (Fig. 5b). Even if sentinel surveillance was conducted at only one tertiary facility, this increase in testing rate

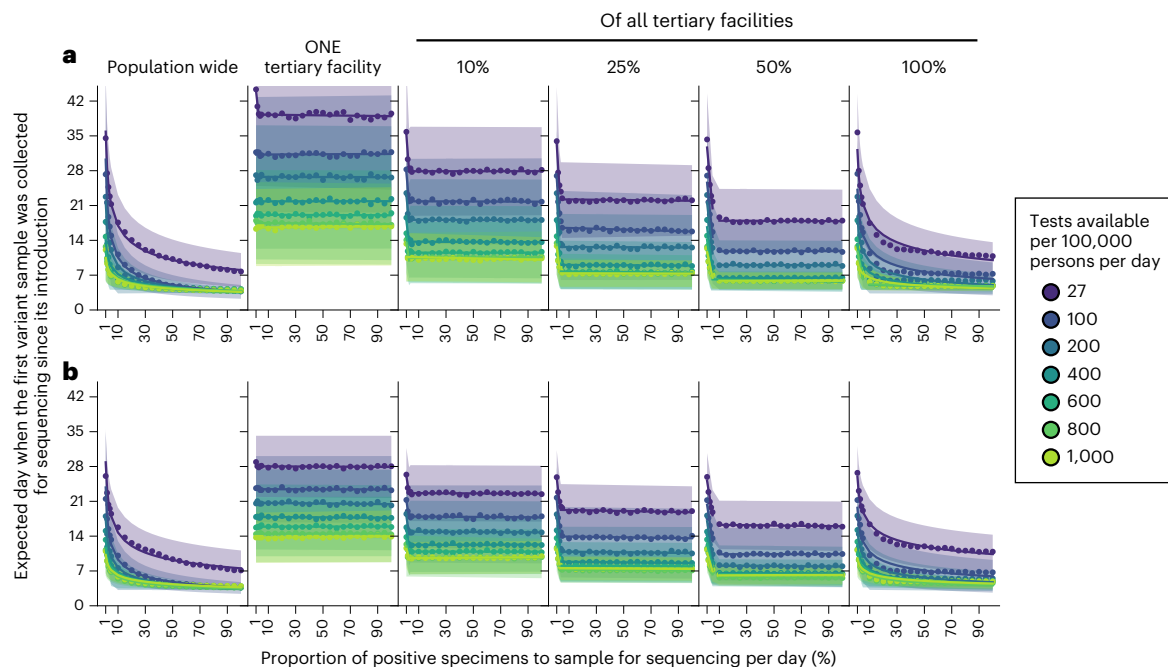


Fig. 3 | Impact of SARS-CoV-2 testing rates and proportion of positive specimens to sequence on variant detection. For each mean daily test availability (differently colored), the expected day (points and line) and the s.d. (shaded region) when the first variant specimen to be sequenced is sampled since its introduction is plotted against the proportion of positive specimens to be sampled for sequencing daily. Different genomic surveillance strategies with varying sampling coverage (that is, all specimens collected from all healthcare

facilities sent to one facility to be sampled for sequencing (population-wide strategy); or only one tertiary facility, or 10, 25, 50 or 100% of tertiary sentinel facilities would sample the specimens they collected for sequencing) were simulated. **a**, Wild-type SARS-CoV-2/Alpha. **b**, Delta/Omicron. The plotted results were computed from 1,000 random independent simulations for each surveillance strategy.

for the catchment area of the facility would likely speed up variant detection by 1–2 weeks.

Second, the representativeness of a specimen pool for sequencing can be further improved by expanding sampling coverage. In our model, variant detection was further sped up by 1–3 weeks by increasing the percentage of tertiary sentinel facilities sending the samples they had collected for sequencing to 25% of facilities (Fig. 5c). Additionally, in terms of prevalence monitoring, if 25% of tertiary facilities sequenced 5% of all positive specimens they had collected to detect and monitor an Alpha-like variant, the maximum absolute difference to the true circulating proportion is expected to decrease from more than 50% (assuming a single sentinel facility) to no more than 20%.

Third, reducing turnaround time from samples referred to sequencing output results in a 1:1 decrease in time to new variant detection, regardless of the proportion of sequenced samples, test availability or sampling coverage (Fig. 5). These gains require scaling up in sample transport networks, access to sequencing machinery, trained personnel and/or increases in numbers of sequenced samples to make the most efficient use of each sequencing run¹¹. Furthermore, LMICs also often face high costs and extended delivery delays of laboratory reagents and consumables that were sometimes further exacerbated by recurring travel bans during the acute phase of the pandemic^{5,12,13}.

After reducing spatiotemporal bias in the specimen pool through increased testing and sampling coverage, sequencing up to 5–10% of the positive specimens collected could return the greatest information gains while minimizing resource wastage. For an Alpha-like variant, 100 tests per 100,000 persons per day with sampling from 25% of tertiary sentinel facilities for sequencing amounts to an estimated 5–10 sequences per week averaged over a 90-day period per 1,000,000 people. If turnaround time is kept within 1 week, the variant would likely be detected within 1 month at a circulating proportion of approximately 4% (Fig. 5d). Similarly, at the same testing rate, sampling

coverage and turnaround time (that is, average 5–11 sequences per week per 1,000,000 people), an Omicron-like variant would be detected before the first month since its introduction, but at approximately 23% circulating proportion owing to its faster transmission (Extended Data Fig. 6).

Our findings serve to inform expectations of genomic surveillance initiatives and should be interpreted according to the public health objectives of each program. If the objective is to serve as an early warning system for the de novo emergence of new variants before they are likely to have spread widely, then all factors above can be considered essential and could require substantially more than 100 tests per 100,000 persons per day. Critically, determining that a new variant is a threat requires not only detection of the variant itself but also the capacity to reliably monitor changes in its prevalence and potential clinical impact on short timescales. The results presented here also inform the design of programs for the sensitive and reliable detection of changes in variant prevalence. Otherwise, if the objective is to detect for the introduction of novel variants from overseas, some of the factors above may be relaxed depending on the public health objectives. For instance, if the aim is to attempt containment, all factors should still be considered to promptly detect and monitor the spread of the variant. However, if the aim is to ensure sufficient time for control strategies to be enacted, less samples could be sequenced or turnaround time could be longer, for example, so long as the mitigation strategies remain useful when implemented.

Despite performing our simulations using demographic parameters from Zambia, the emergence and detection of each VOC to date represents interesting case studies for the work described here (see ‘Emergence of SARS-CoV-2 variants of concern’ in Supplementary Notes). For example, at the time of the first detection of the Omicron variant, in South Africa in November 2021, the daily SARS-CoV-2 testing rate was 51 tests per 100,000 people per day⁹, which was among the

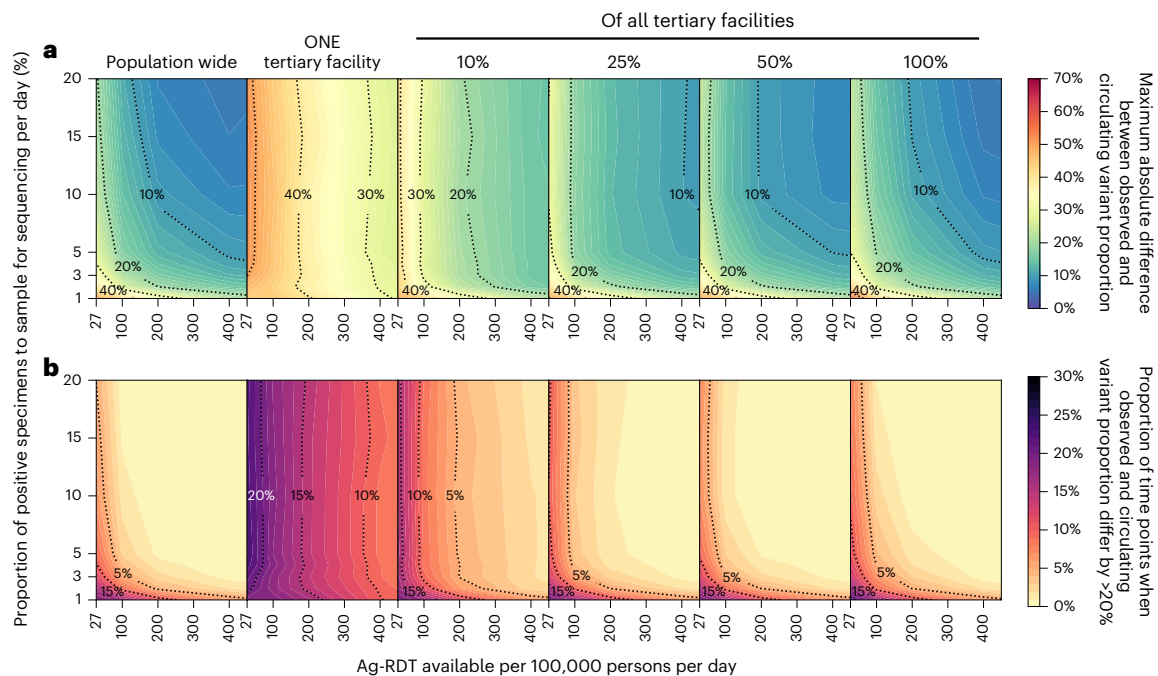


Fig. 4 | Impact of SARS-CoV-2 testing rates on the capacity to monitor changes in variant prevalence based on diagnostic test availability and proportion of test-positive samples sequenced. Different genomic surveillance strategies (that is, all specimens collected from all healthcare facilities sent to one facility to be sampled for sequencing (population-wide strategy); or only one tertiary facility or 10, 25, 50 or 100% of tertiary sentinel

facilities would sample the specimens they collected for sequencing) were simulated. **a**, Maximum absolute difference between observed and circulating variant proportions. **b**, Proportion of time points when sequencing was performed that the absolute difference between observed and circulating variant proportions is greater than 20%. All results were computed from 1,000 random independent simulations for each surveillance strategy.

highest testing rates in Africa. However, the Omicron variant was only detected 6–8 weeks after its likely emergence⁴. At that point, Omicron had already infected a substantial portion of the population in Gauteng, South Africa (that is, the estimated circulating variant proportion was greater than 80% by mid-November)⁴. Not only had the variant already spread across the rest of South Africa and to neighboring Botswana⁴, Omicron samples were also collected in multiple other countries, including Hong Kong¹⁴, Denmark¹⁵ and the Netherlands¹⁶, before the initial reports on the identification of the Omicron variant. This situation is consistent with our modeling findings, where novel variant detection is possible with less than 100 tests per 100,000 persons per day, but only after the new variant has spread widely across the population.

In another example, Germany randomly sequenced approximately 60–70 sequences per week (that is, less than 1% of cases sequenced per day) in December 2020¹⁷. During this time, testing rates in Germany averaged at approximately 300 tests per 100,000 persons per day⁹. Germany was able to detect the Alpha variant 1 week before the World Health Organization declared the lineage a VOC in mid-December 2020¹⁷. The Alpha variant likely emerged in the UK in mid-September 2020¹⁸ and rapidly proliferated across the country before it was reported in December 2020¹⁹. Our analyses showed that the expected time before the first Alpha variant specimen was sampled for sequencing since its introduction is more than 4 weeks (that is, around November 2020) at Germany's testing and sequencing rate. This falls in line with the likely period of Alpha's introduction into Germany, similar to the period estimated for its European neighbors, such as the Netherlands²⁰.

There are some limitations to our work. First, although we computed the amount of testing and sampling coverage required to achieve prompt and precise variant surveillance outcomes, comprehensive cost-effectiveness analyses are needed to determine the cost-optimal approach toward expanding testing programs that support surveillance alongside other epidemic control objectives.

Second, PATAT iteratively simulates the course of an epidemic wave in time steps of 1 day. As a simplification, PATAT assumes a logical flow where testing and isolation after positive diagnoses occur before transmissions are simulated each day. However, in reality, transmission could occur before testing and isolation and thus potentially lead to an underestimation in infections. Nonetheless, a substantial portion of SARS-CoV-2 transmissions are attributable to individuals who are asymptomatic and presymptomatic²¹, who would not seek testing until they present symptoms. This was reflected in our simulations (Extended Data Fig. 7). As such, it is unlikely our simulations substantially underestimate disease spread. Furthermore, other agent-based SARS-CoV-2 transmission models that made similar assumptions were validated against real-world epidemiological data^{22,23}. Importantly, our simulation results also fit well against confirmed case and death counts in Zambia when accounting for the prevailing testing rates in the country (see 'Model validation' in Supplementary Notes and Extended Data Fig. 8).

Although we find that routine representative sampling is vital for monitoring SARS-CoV-2 evolution, additional surveillance systems, including targeted surveillance of particular populations and settings (such as individuals who are immunocompromised or unusual events) and wastewater sampling, could enable increased variant detection sensitivity²⁴. In particular, recent advances in wastewater sequencing and deconvolution methods to resolve multiple viral lineages in mixed wastewater samples enabled detection of emerging variants before they were captured by clinical genomic surveillance^{25–27}. However, sequence quality is often poor in wastewater samples and, in turn, these methods depend on a priori knowledge of the lineage-defining mutations of VOCs and variants of interest, which are currently still identified based on notable upsurges in individuals with clinical diagnoses. Furthermore, centralized wastewater management systems, which these methods rely on for accurate determination of relative lineage prevalence, are currently nonexistent in many LMICs. Substantial

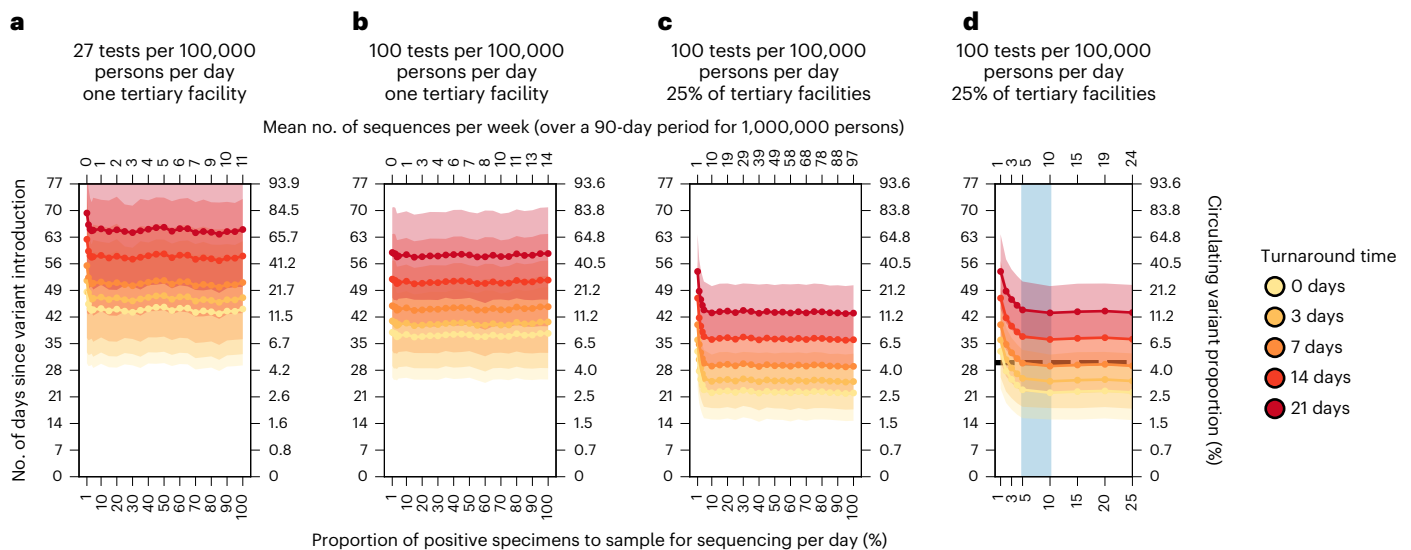


Fig. 5 | Recommended approach to enhance genomic surveillance robustness. In each plot, the operating curves of the expected day when the first Alpha variant sequence is generated are plotted for different proportions of specimens to sample for sequencing per day and turnaround times. We assumed that the Alpha variant was circulating at 1% initially, with wild-type SARS-CoV-2 in the background. We also assumed that positive specimens sampled within each week for sequencing are consolidated into a batch before they are referred for sequencing. Turnaround time refers to the time between collection of each weekly consolidated batch of positive specimens to the acquisition of its corresponding sequencing data. The vertical axes denote the number of days passed since the introduction of the Alpha variant (left) and its corresponding circulating proportion (right). The horizontal axes denote the proportion of positive specimens to sample for sequencing per day (bottom)

and the corresponding mean number of sequences to be generated per week per 1,000,000 people over a 90-day epidemic period. **a**, Specimen pools for sequencing from *one* tertiary sentinel facility with testing rate at 27 tests per 100,000 persons per day. **b**, Specimen pools for sequencing from *one* tertiary sentinel facility with testing rate at 100 tests per 100,000 persons per day. **c**, Specimen pools for sequencing from 25% of all tertiary sentinel facilities with testing rate at 100 tests per 100,000 per day. **d**, Zoomed-in plot of **c** to highlight sequencing proportions varying between 1 and 25%. Sequencing 5–10% of positive specimens (blue shaded region) would ensure that we would expect to detect Alpha in 30 days (horizontal dashed line) if turnaround time is kept within 1 week. All results were computed from 1,000 random independent simulations for each surveillance strategy. The shaded region depicts the s.d. across simulations.

investments, coordination and time are needed to enable local sanitation infrastructures suitable for wastewater surveillance²⁸. Detection of genetic markers, such as *S*-gene target failure in PCR assays, may also provide faster notification of viral lineages with these specific mutations. However, whole-genome sequencing is still needed for unambiguous genotyping of SARS-CoV-2 samples. Ultimately, clinical diagnostic testing and surveillance will remain the core mode of SARS-CoV-2 surveillance in most countries.

During the initial phase of the pandemic in 2020, due to limited testing and sequencing capacities, many LMICs were initially focused on genomic surveillance efforts at points of entry at country borders to deter introductions^{29–31}. Over time, especially after the emergence of VOCs, SARS-CoV-2 genomic surveillance gradually expanded to include community surveillance as many LMICs enhanced their sequencing capacities^{4,31–33}. This was done either by establishing regional sequencing networks to maximize available resources, investing in local sequencing capacities or partnering with global collaborators^{33–35}. Sequencing turnaround time has also improved from an average of approximately 170 days in 2020 to approximately 30 days in 2021 across the African continent, albeit with substantial variation among countries³³. Although sequencing capabilities have expanded in LMICs, obtaining spatiotemporally representative samples remains a key challenge³³. Our work shows that the sensitivity of genomic surveillance programs is highly dependent on diagnostic testing rate and that a mean testing rate of 100 tests per 100,000 persons per day at sentinel sites that are geographically spread out across the community is a good basis for monitoring virus variants. Whereas a reflexive PCR test after a positive Ag-RDT diagnosis is currently performed to obtain samples suitable for sequencing (and is possible in many tertiary facilities in LMICs), this presents additional cost and logistical

barriers. Recent studies showed that SARS-CoV-2 sequencing can be performed using materials obtained from Ag-RDTs performed at point of care^{36–38}. Importantly, whole genomes can be recovered up to 8 days after testing, providing opportunities for sequencing to be performed on samples performed through self-testing as well³⁶.

Expanding genomic sequencing capabilities, especially in LMICs, is a global priority³⁹ and current investments in sequencing must continue^{33,34}. Simultaneously, sustained investments in public health systems are required to expand access to, and availability of, diagnostic testing to underpin SARS-CoV-2 surveillance programs. Here, we primarily focused on LMICs, but our findings on the impact of testing rates and representativeness on genomic surveillance programs are equally important for HICs as parts of their testing and surveillance infrastructures are dismantled following the acute health emergency of the COVID-19 pandemic. Ultimately, detecting the next SARS-CoV-2 variant or pathogen that causes the next pandemic requires fundamental clinical diagnostic capacity to monitor existing and emerging pathogens.

Online content

Any methods, additional references, Nature Portfolio reporting summaries, source data, extended data, supplementary information, acknowledgements, peer review information; details of author contributions and competing interests; and statements of data and code availability are available at <https://doi.org/10.1038/s41588-022-01267-w>.

References

1. Robishaw, J. D. et al. Genomic surveillance to combat COVID-19: challenges and opportunities. *Lancet Microbe* **2**, e481–e484 (2021).

2. Davies, N. G. et al. Estimated transmissibility and impact of SARS-CoV-2 lineage B.1.1.7 in England. *Science* **372**, eabg3055 (2021).
3. Cherian, S. et al. SARS-CoV-2 spike mutations, L452R, T478K, E484Q and P681R, in the second wave of COVID-19 in Maharashtra, India. *Microorganisms* **9**, 1542 (2021).
4. Viana, R. et al. Rapid epidemic expansion of the SARS-CoV-2 Omicron variant in southern Africa. *Nature* **603**, 679–686 (2022).
5. Brito, A. F. et al. Global disparities in SARS-CoV-2 genomic surveillance. *Nat. Commun.* **13**, 7003 (2022).
6. Wohl, S., Lee, E. C., DiPrete, B. L. & Lessler, J. Sample size calculations for variant surveillance in the presence of biological and systematic biases. Preprint at *medRxiv* <https://doi.org/10.1101/2021.12.30.21268453> (2022).
7. *Sequencing of SARS-CoV-2 - first update*. (European Centre for Disease Prevention and Control, 2022); <https://www.ecdc.europa.eu/en/publications-data/sequencing-sars-cov-2>
8. *Guidance for surveillance of SARS-CoV-2 variants: interim guidance, 9 August 2021* (World Health Organization, 2021); <https://apps.who.int/iris/handle/10665/343775>
9. FIND SARS-COV-2 Test tracker. *FIND* <https://www.finndx.org/covid-19/test-tracker/> (2022).
10. Ferguson, N. et al. Growth, population distribution and immune escape of Omicron in England - Report 49 (Imperial College London, 2021); <https://www.imperial.ac.uk/mrc-global-infectious-disease-analysis/covid-19/report-49-omicron/>
11. Inzaule, S. C., Tessema, S. K., Kebede, Y., Ogwel Ouma, A. E. & Nkengasong, J. N. Genomic-informed pathogen surveillance in Africa: opportunities and challenges. *Lancet Infect. Dis.* **21**, e281–e289 (2021).
12. Mallapaty, S. Omicron-variant border bans ignore the evidence, say scientists. *Nature* **600**, 199 (2021).
13. Merhi, G. et al. SARS-CoV-2 genomic epidemiology: data and sequencing infrastructure. *Future Microbiol* **17**, 1001–1007 (2022).
14. Gu, H. et al. Probable transmission of SARS-CoV-2 Omicron variant in quarantine hotel, Hong Kong, China, November 2021. *Emerg. Infect. Dis.* **28**, 460 (2022).
15. Espenhain, L. et al. Epidemiological characterisation of the first 785 SARS-CoV-2 Omicron variant cases in Denmark, December 2021. *Eurosurveillance* **26**, 2101146 (2021).
16. Rijksinstituut voor Volksgezondheid en Milieu Omicron variant found in two previous test samples. <https://www.rivm.nl/en/news/omicron-variant-found-in-two-previous-test-samples> (2021).
17. Oh, D. Y. et al. Advancing precision vaccinology by molecular and genomic surveillance of severe acute respiratory syndrome coronavirus 2 in Germany, 2021. *Clin. Infect. Dis.* **75**, S110–S120 (2022).
18. Hill, V. et al. The origins and molecular evolution of SARS-CoV-2 Lineage B.1.1.7 in the UK. *Virus Evol.* **8**, veac080 (2022).
19. Volz, E. et al. Assessing transmissibility of SARS-CoV-2 lineage B.1.1.7 in England. *Nature* **593**, 266–269 (2021).
20. Han, A. X. et al. Regional importation and asymmetric within-country spread of SARS-CoV-2 variants of concern in the Netherlands. *eLife* **11**, e78770 (2022).
21. Moghadas, S. M. et al. The implications of silent transmission for the control of COVID-19 outbreaks. *Proc. Natl Acad. Sci. USA* **117**, 17513–17515 (2020).
22. Kerr, C. C. et al. Covasim: an agent-based model of COVID-19 dynamics and interventions. *PLoS Comput. Biol.* **17**, e1009149 (2021).
23. López, J. A. M. et al. Anatomy of digital contact tracing: Role of age, transmission setting, adoption, and case detection. *Sci Adv* **7**, eabd8750 (2021).
24. Knyazev, S. et al. Unlocking capacities of genomics for the COVID-19 response and future pandemics. *Nat. Methods* **19**, 374–380 (2022).
25. Karthikeyan, S. et al. Wastewater sequencing reveals early cryptic SARS-CoV-2 variant transmission. *Nature* **609**, 101–108 (2022).
26. Baaijens, J. A. et al. Lineage abundance estimation for SARS-CoV-2 in wastewater using transcriptome quantification techniques. *Genome Biol.* **23**, 236 (2022).
27. Jahn, K. et al. Early detection and surveillance of SARS-CoV-2 genomic variants in wastewater using COJAC. *Nat. Microbiol* **7**, 1151–1160 (2022).
28. Shrestha, S. et al. Wastewater-based epidemiology for cost-effective mass surveillance of COVID-19 in low- and middle-income countries: challenges and opportunities. *Water* **13**, 2897 (2021).
29. Butera, Y. et al. Genomic sequencing of SARS-CoV-2 in Rwanda reveals the importance of incoming travelers on lineage diversity. *Nat. Commun.* **12**, 5705 (2021).
30. Salyer, S. J. et al. The first and second waves of the COVID-19 pandemic in Africa: a cross-sectional study. *Lancet* **397**, 1265–1275 (2021).
31. Morang'a, C. M. et al. Genetic diversity of SARS-CoV-2 infections in Ghana from 2020–2021. *Nat. Commun.* **13**, 2494 (2022).
32. Cowley, L. A. et al. Genomics, social media and mobile phone data enable mapping of SARS-CoV-2 lineages to inform health policy in Bangladesh. *Nat. Microbiol* **6**, 1271–1278 (2021).
33. Tegally, H. et al. The evolving SARS-CoV-2 epidemic in Africa: insights from rapidly expanding genomic surveillance. *Science* **378**, eabq5358 (2022).
34. Leite, J. A. et al. Implementation of a COVID-19 genomic surveillance regional network for Latin America and Caribbean region. *PLoS ONE* **17**, e0252526 (2022).
35. Dhar, M. S. et al. Genomic characterization and epidemiology of an emerging SARS-CoV-2 variant in Delhi, India. *Science* **374**, 995–999 (2021).
36. Martin, G. E. et al. Maintaining genomic surveillance using whole-genome sequencing of SARS-CoV-2 from rapid antigen test devices. *Lancet Infect. Dis.* **22**, 1417–1418 (2022).
37. Nazario-Toole, A. et al. Sequencing SARS-CoV-2 from antigen tests. *PLoS ONE* **17**, e0263794 (2022).
38. Macori, G. et al. Inactivation and recovery of high quality RNA from positive SARS-CoV-2 rapid antigen tests suitable for whole virus genome sequencing. *Front Public Health* **10**, 1135 (2022).
39. Adepoju, P. Challenges of SARS-CoV-2 genomic surveillance in Africa. *Lancet Microbe* **2**, e139 (2021).

Publisher's note Springer Nature remains neutral with regard to jurisdictional claims in published maps and institutional affiliations.

Open Access This article is licensed under a Creative Commons Attribution 4.0 International License, which permits use, sharing, adaptation, distribution and reproduction in any medium or format, as long as you give appropriate credit to the original author(s) and the source, provide a link to the Creative Commons license, and indicate if changes were made. The images or other third party material in this article are included in the article's Creative Commons license, unless indicated otherwise in a credit line to the material. If material is not included in the article's Creative Commons license and your intended use is not permitted by statutory regulation or exceeds the permitted use, you will need to obtain permission directly from the copyright holder. To view a copy of this license, visit <http://creativecommons.org/licenses/by/4.0/>.

© The Author(s) 2023

Methods

Simulating SARS-CoV-2 epidemics with the PATAT model

We used PATAT, a stochastic, individual-based model to simulate SARS-CoV-2 epidemics in a community with demographic profiles, contact mixing patterns and level of public health resources mirroring those typically observed in LMICs. Here, the model was based on Zambia. PATAT creates an age-structured population, linking individuals within contact networks of multigenerational households, schools, workplaces and churches (that is, regular mass gatherings) (Supplementary Table 1). The simulated number of healthcare facilities (that is, community clinics and tertiary hospitals) where individuals with mild symptoms seek symptomatic testing and have their virus specimens collected was based on an empirical clinic to population ratio (that is, one healthcare facility for every 7,000 individuals, on average)^{40,41}. Although PATAT does not explicitly simulate the spatial location of individuals, contact networks and healthcare facilities are ordered to approximate localized community structures (that is, the closer the number order of a facility, the closer they are in the same neighborhood) that is most illustrative of urban centers. Households are proximally ordered and distributed around these facilities based on an empirical distance-structured distribution that correlates with probabilities of individuals with symptoms seeking testing at clinics (Supplementary Table 1).

We then simulated SARS-CoV-2 infection waves in a population of 1,000,000 individuals over a 90-day period that begins with an initial 1% prevalence of an extant SARS-CoV-2 variant and the introduction of a mutant variant at 0.01%. We assumed that clinic-based, professional-use Ag-RDTs are the predominant SARS-CoV-2 diagnostic used for SARS-CoV-2 testing³⁹. Because Ag-RDT sensitivity depends on within-host viral loads⁴², PATAT generates viral load trajectories, measured in cycle threshold values, for individuals with COVID-19 by randomly sampling from known viral load distributions of different SARS-CoV-2 variants^{43,44}. We performed simulations for two variant replacement scenarios, Alpha variant introduction while the wild-type virus was circulating (wild-type/Alpha) and Omicron (BA.1) variant introduction while Delta was circulating (Delta/Omicron), applying known distributions of their peak viral load, incubation and virus clearance periods^{43,45} (Supplementary Table 1). Before simulating the two-variant epidemic, we first calibrated the transmission probability parameter for the extant variant such that it would spread in a completely susceptible population at $R_0 = 2.5-3.0$. We then assumed Alpha and Omicron (BA.1) were more transmissible than the respective extant virus to achieve growth rates of approximately 0.15 and 0.35 per day, respectively^{2,10}.

For both sets of simulations, we assumed that 10% of the population had infection-acquired immunity against the extant strain initially, with some level of protection against infection by the mutant virus (wild-type SARS-CoV-2, 80% protection against Alpha⁴⁶; Delta, 20% protection against Omicron¹⁰). We also investigated the scenario where 40% of the population had infection-acquired immunity as part of sensitivity analyses (see below). We did not investigate scenarios involving vaccine-acquired immunity due to low vaccine uptake in most LMICs⁴⁷.

PATAT uses the SEIRD (susceptible-exposed-infected-recovered/death) epidemic model for disease progression and stratifies individuals who are infected on the basis of their symptom presentation (asymptomatic, mild or severe). After an assumed random delay after symptom onset (mean = 1 day; s.d. = 0.5 day), individuals with symptoms who seek testing would do so at their nearest healthcare facility, where test-positive samples may be reflexively collected for sequencing. We assumed that individuals with symptoms sought testing based on a probability distribution of health service-seeking behavior that inversely correlates with the distance between the individual's household and the nearest healthcare facility (Supplementary Table 1)⁴⁸.

We varied levels of Ag-RDT stocks per day (that is, 27, 100 and 200–1,000 (in increments of 200) tests per 100,000 persons per day), running ten independent epidemic simulations for each testing rate.

Given the start of a week on a Monday, we assumed that a week's worth of tests are delivered to healthcare facilities every Monday and unused Ag-RDTs in the previous week are carried forward into the next week. If test stocks for a particular week were exhausted before the end of the week, testing for the rest of that week ceased. Due to overlapping symptoms between COVID-19 and other respiratory diseases, a proportion of available Ag-RDTs would be used by individuals who are not infected with SARS-CoV-2. Based on test positivity rates reported by various countries in the second half of 2021⁴⁹, we assumed a 10% test positivity rate at the start and end of the simulated epidemic, and 20% test positivity at its peak, linearly interpolating the rates between these time points. We also assumed that false-positive specimens could be sampled based on a reported Ag-RDT specificity of 98.9%⁴².

We assumed that any specimens collected for genomic surveillance after positive detection through Ag-RDT would be reflexively confirmed with PCR. We also assumed that all individuals who were symptomatic with severe symptoms require hospitalization, and are tested separately from persons with mild symptoms who sought testing. Given that likely only approximately 10–20% of people who died from COVID-19 in Zambia were tested for the disease in life^{50,51}, we assumed that only 20% of individuals with severe disease would be tested by Ag-RDT or PCR upon presenting severe symptoms and have specimens collected for sequencing.

Full technical details of PATAT are described in the Supplementary Information. The full model source code is available at <https://github.com/AMC-LAEB/PATAT-sim>.

Genomic surveillance strategies

Twenty percent of healthcare facilities were assumed to be tertiary facilities based on empirical data collected from Zambia^{40,41}. We assumed that tertiary facilities provide testing for individuals with mild symptoms and hospitalized patients with severe symptoms. Given that healthcare facilities were proximally ordered, we randomly selected tertiary facilities in each independent surveillance simulation (see below), but ensured that the selected facilities were not consecutively ordered. In sum, all tertiary facilities accounted for a median of 18.4% (interquartile range = 17.7–19.1%) of total testing volume across all simulations. We assumed that a proportion of tertiary facilities serve as sentinel surveillance sites that reflexively collect SARS-CoV-2-positive samples for sequencing. We then simulated six strategies with varying degrees of sampling coverage, where positive specimens collected from testing sites would be consolidated and sampled for sequencing: (1) all samples from community clinics and tertiary hospitals are sent to a centralized facility and further sampled for sequencing (that is, population-wide strategy); (2) only one tertiary sentinel facility for the population of 1,000,000 simulated people would sequence a portion of positive specimens it has collected, both from individuals with mild symptoms seeking symptomatic testing and individuals with severe symptoms who sought tertiary care at the facility; or only (3) 10%, (4) 25%, (5) 50% and (6) 100% of all tertiary sentinel facilities would sample and sequence a proportion of the specimens they have collected.

For all strategies, we assumed that a proportion (1–100%; in 2% increments between 1 and 5%, in 5% increments between 5 and 100%) of positive specimens are collected daily for sequencing. We also assumed that positive specimens sampled within each week for sequencing are consolidated into a batch before they are referred for sequencing. Turnaround time refers to the time between collection of each weekly consolidated batch of positive specimens to the acquisition of its corresponding sequencing data. Because the within-host viral loads of individuals infected with SARS-CoV-2 were simulated, we assumed that only high-quality samples, where cycle threshold values less than 30, could be sequenced and that the sequencing success rate is 80%, as assumed in other studies⁶.

For each strategy and sequencing proportion, we performed 100 independent surveillance simulations for each epidemic simulation

with a given test stock availability, thus totaling to 1,000 random simulations for each set of variables (that is, testing rate, sequencing proportion and strategy).

Statistics and reproducibility

No statistical method was used to predetermine the population size in our agent-based modeling study. We chose to simulate a population size of 1,000,000 individuals because it is sufficiently large enough to generate the desired epidemic characteristics and inferences on surveillance outcomes. We validated our simulation results based on this population size against real-life reported case count data in Zambia (see ‘Model validation’ in Supplementary Notes). All simulation data generated were included in our analyses.

Ethics statement

Ethics approval was not required for this study.

Reporting summary

Further information on research design is available in the Nature Portfolio Reporting Summary linked to this article.

Data availability

Data on global testing rates were downloaded from <https://www.finddx.org/covid-19/test-tracker>. All data used to parameterize the PATAT simulation model can be found in the article and Supplementary Information. All simulation data generated for this study can be found in the GitHub repository (<https://github.com/AMC-LAEB/PATAT-sim>).

Code availability

The PATAT model source code and custom codes used to analyze our simulation data are available at <https://github.com/AMC-LAEB/PATAT-sim> and https://github.com/AMC-LAEB/PATAT-sim/blob/main/projects/surveillance/han-et-al_genome_surveillance_lmics.ipynb, respectively. This version of the model and analysis codes is also available at <https://doi.org/10.5281/zenodo.7308781>.

References

40. Girdwood, S. J. et al. Optimizing viral load testing access for the last mile: geospatial cost model for point of care instrument placement. *PLoS ONE* **14**, e0221586 (2019).
41. Nichols, B. E. et al. Monitoring viral load for the last mile: what will it cost? *J. Int AIDS Soc.* **22**, e25337 (2019).
42. Brümmer, L. E. et al. Accuracy of novel antigen rapid diagnostics for SARS-CoV-2: a living systematic review and meta-analysis. *PLoS Med.* **18**, e1003735 (2021).
43. Linton, N. M. et al. Incubation period and other epidemiological characteristics of 2019 novel coronavirus infections with right truncation: a statistical analysis of publicly available case data. *J. Clin. Med.* **9**, 538 (2020).
44. Kissler, S. M. et al. Viral dynamics of acute SARS-CoV-2 infection and applications to diagnostic and public health strategies. *PLoS Biol.* **19**, e3001333 (2021).
45. Hay, J. A. et al. Quantifying the impact of immune history and variant on SARS-CoV-2 viral kinetics and infection rebound: A retrospective cohort study. *eLife* **11**, e81849 (2022).
46. Pouwels, K. B. et al. Effect of Delta on viral burden and vaccine effectiveness against new SARS-CoV-2 infections in the UK. *Nat. Med.* **27**, 2127–2135 (2021).
47. Mathieu, E. et al. A global database of COVID-19 vaccinations. *Nat. Hum. Behav.* **5**, 947–953 (2021).

48. Dovel, K. et al. Frequency of visits to health facilities and HIV services offered to men, Malawi. *Bull. World Health Organ* **99**, 618–626 (2021).
49. Hasell, J. et al. A cross-country database of COVID-19 testing. *Sci. Data* **7**, 345 (2020).
50. Mwananyanda, L. et al. Covid-19 deaths in Africa: prospective systematic postmortem surveillance study. *Brit. Med. J.* **372**, n334 (2021).
51. Gill, C. J. et al. What is the prevalence of COVID-19 detection by PCR among deceased individuals in Lusaka, Zambia? A postmortem surveillance study. *BMJ Open* **12**, e066763 (2022).

Acknowledgements

We are pleased to acknowledge that all computational work reported in this paper was performed on the Shared Computing Cluster, which is administered by Boston University’s Research Computing Services (www.bu.edu/tech/support/research/). This work was supported by the Rockefeller Foundation, and the Governments of Germany, Canada, UK, Australia, Norway, Saudi Arabia, Kuwait, the Netherlands and Portugal. A.X.H. and C.A.R. were supported by European Research Council NaviFlu (grant 818353). C.A.R. was also supported by a National Institutes of Health R01 grant (5R01AI132362-04) and a Dutch Research Council (NWO) Vici Award (09150182010027). The funders had no role in study design, data collection and analysis, decision to publish or preparation of the manuscript. The findings and conclusions in this manuscript are those of the authors and do not represent the official position of the World Health Organization.

Author contributions

A.X.H., B.E.N., C.A.R., J.A.S., M.D.P., S.B., M.v.K., A.T., E.H., S.C. and B.R. contributed to conceptualization. A.X.H., B.E.N. and C.A.R. wrote the original draft and contributed to methodology, formal analysis and data curation. A.X.H. contributed to software. A.X.H., E.P., B.E.N. and C.A.R. contributed to validation and visualization. A.X.H., B.E.N., C.A.R., J.A.S., M.P., S.B. and M.v.K. contributed to investigation. B.E.N., C.A.R., A.T., E.H., S.C. and B.R. contributed to resources. B.E.N. and C.A.R. provided supervision and contributed to project administration. B.E.N., C.A.R., A.T., E.H., S.C. and B.R. contributed to funding acquisition. All authors reviewed and edited the manuscript.

Competing interests

A.T., E.H., S.C., B.R. and B.E.N. declare that they are employed by FIND, the global alliance for diagnostics. All remaining authors declare no competing interests.

Additional information

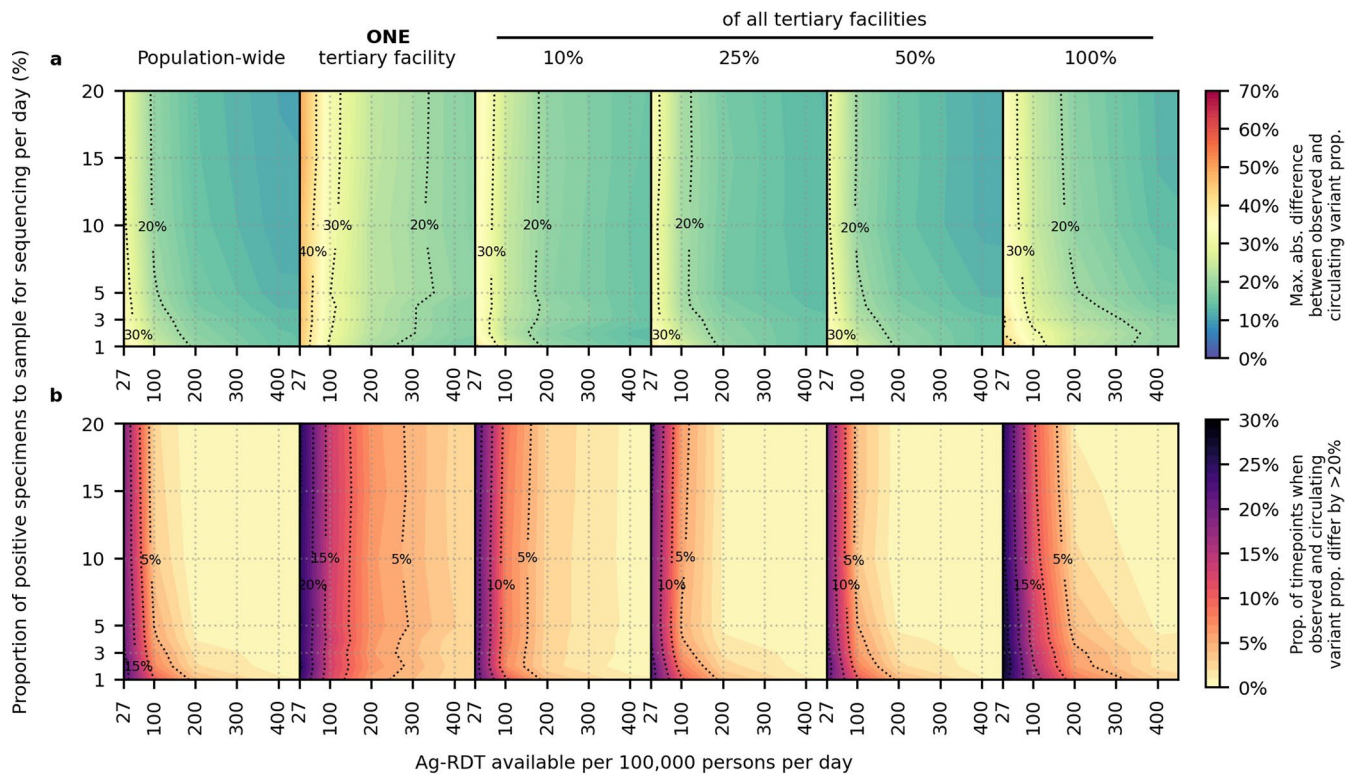
Extended data is available for this paper at <https://doi.org/10.1038/s41588-022-01267-w>.

Supplementary information The online version contains supplementary material available at <https://doi.org/10.1038/s41588-022-01267-w>.

Correspondence and requests for materials should be addressed to Alvin X. Han or Colin A. Russell.

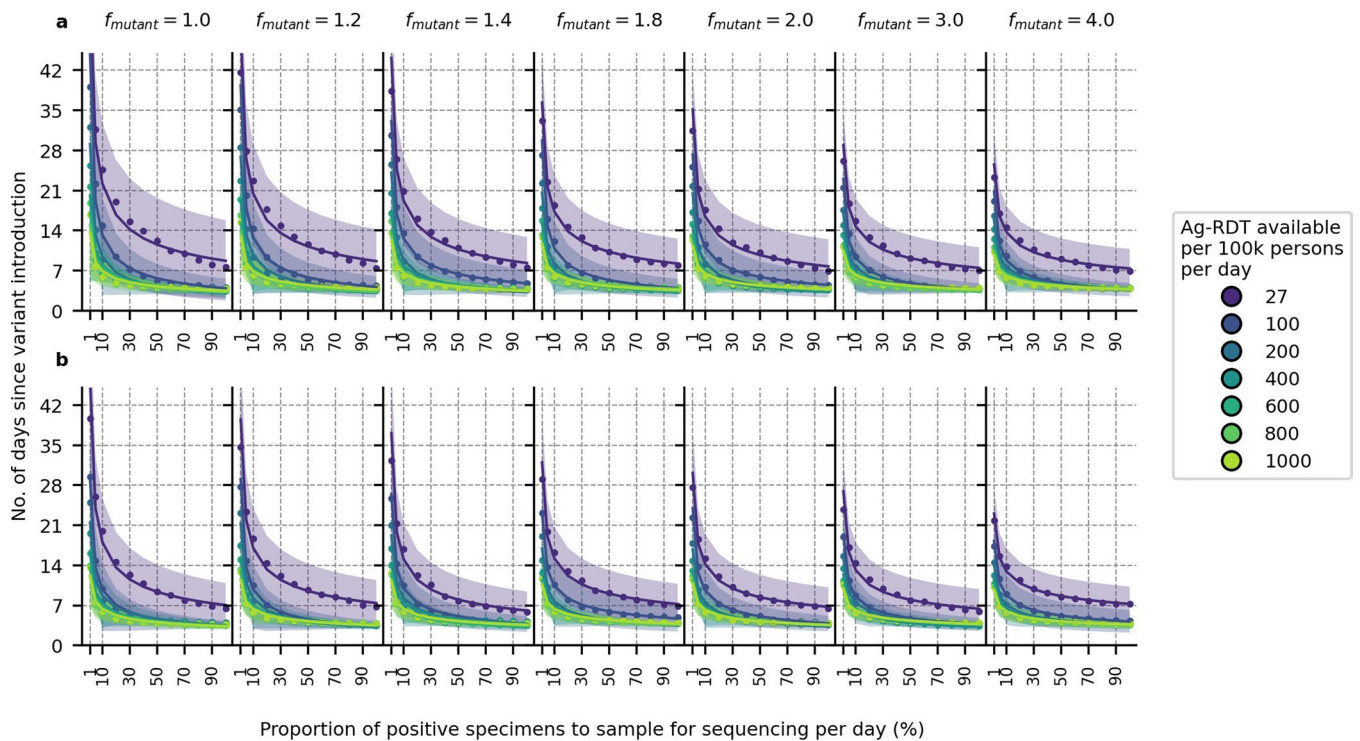
Peer review information *Nature Genetics* thanks Gordon Awandare and the other, anonymous, reviewer(s) for their contribution to the peer review of this work.

Reprints and permissions information is available at www.nature.com/reprints.



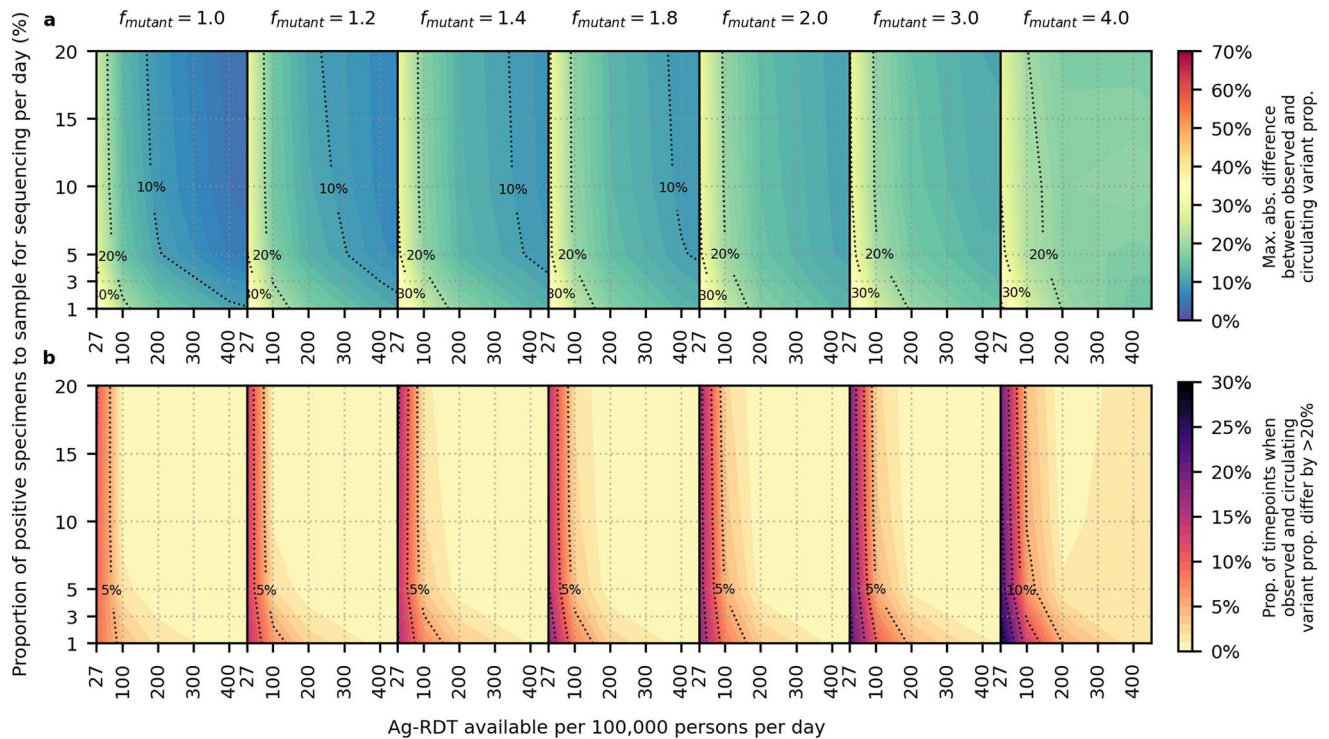
Extended Data Fig. 1 | Impact of SARS-CoV-2 Ag-RDT testing rates and daily proportion of positive specimens to sample for sequencing on observed Omicron variant proportions. Different genomic surveillance strategies (that is all specimens collected from all healthcare facilities sent to one facility to be sampled for sequencing (*population-wide* strategy); only *one*, 10%, 25%, 50% or 100% of all tertiary facilities acting as sentinel sites that would sample

the specimens they collected for sequencing) were simulated. **(A)** Maximum absolute difference between observed and circulating variant proportions. **(B)** Proportion of timepoints when sequencing was performed that the absolute difference between observed and circulating variant proportions is greater than 20%. All results were computed from 1,000 random independent simulations for each surveillance strategy.



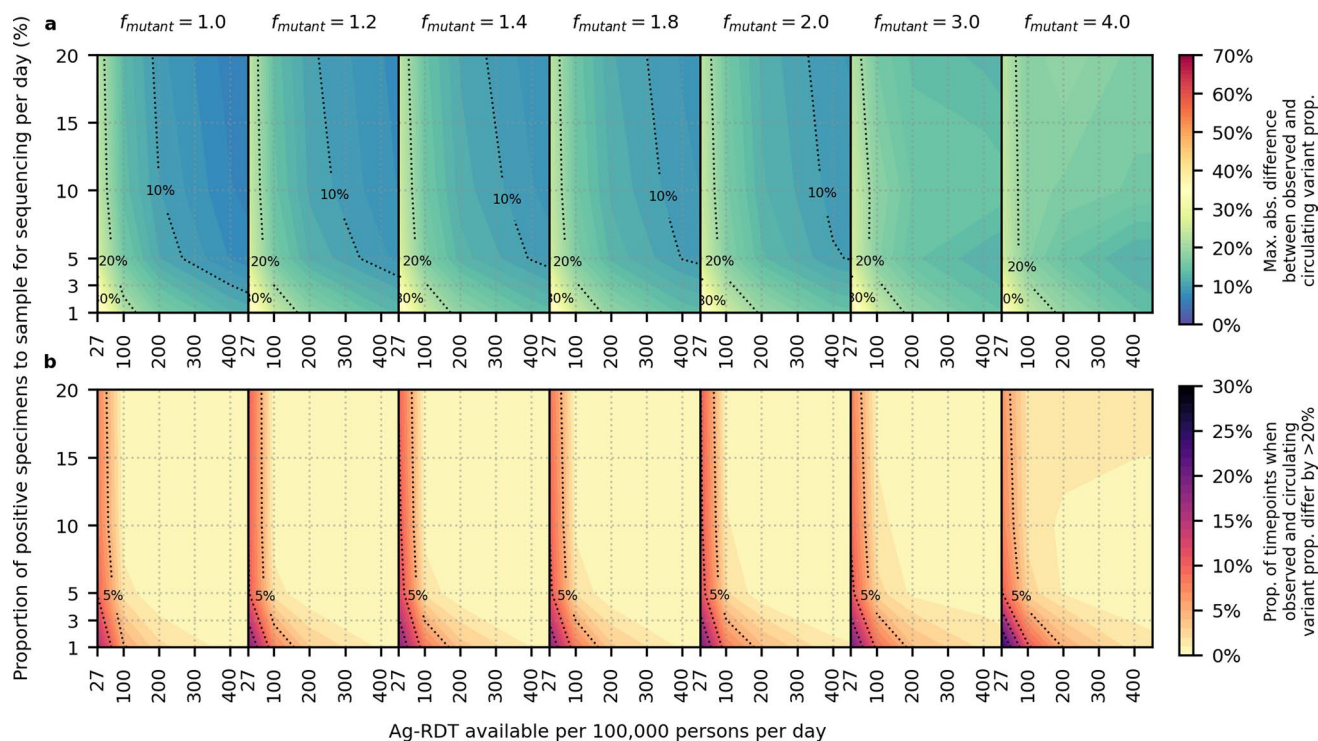
Extended Data Fig. 2 | Sensitivity analyses on variant detection operating curve for different relative transmissibility factor. For each Ag-RDT availability (differently colored), the expected day (points and line) and the standard deviation (shaded region) when the first Omicron variant specimen (in the background of extant Delta variant) is sampled for sequencing since its introduction is plotted against the proportion of positive specimens to be sampled for sequencing daily. All specimens collected from the population from

all healthcare facilities were sent to one facility to be sampled for sequencing (population-wide genomic surveillance strategy). Different transmissibility factor of Omicron relative to Delta (f_{mutant}) were assumed. **(A)** 10% and **(B)** 40% of the population had immunity against Omicron initially. The plotted results were computed from 1,000 random independent simulations for each surveillance strategy.



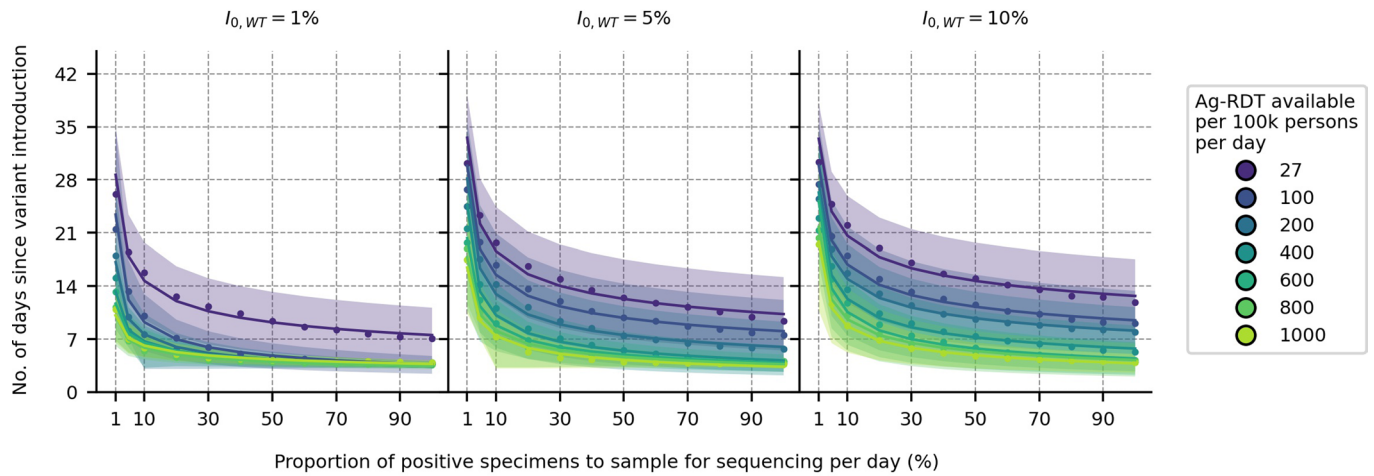
Extended Data Fig. 3 | Sensitivity analyses on accuracy of observed variant proportions for different relative transmissibility factor. Omicron-like virus properties assumed for variant and initial proportion of population with some degree of protection against the variant virus assumed at 10%. All specimens collected from the population from all healthcare facilities were sent to one facility to be sampled for sequencing (population-wide genomic surveillance

strategy). Different transmissibility factor of Omicron relative to Delta (f_{mutant}) were assumed. **(A)** Maximum absolute difference between observed and circulating variant proportions. **(B)** Proportion of timepoints when sequencing was performed that the absolute difference between observed and circulating variant proportions is greater than 20%. All results were computed from 1,000 random independent simulations for each surveillance strategy.



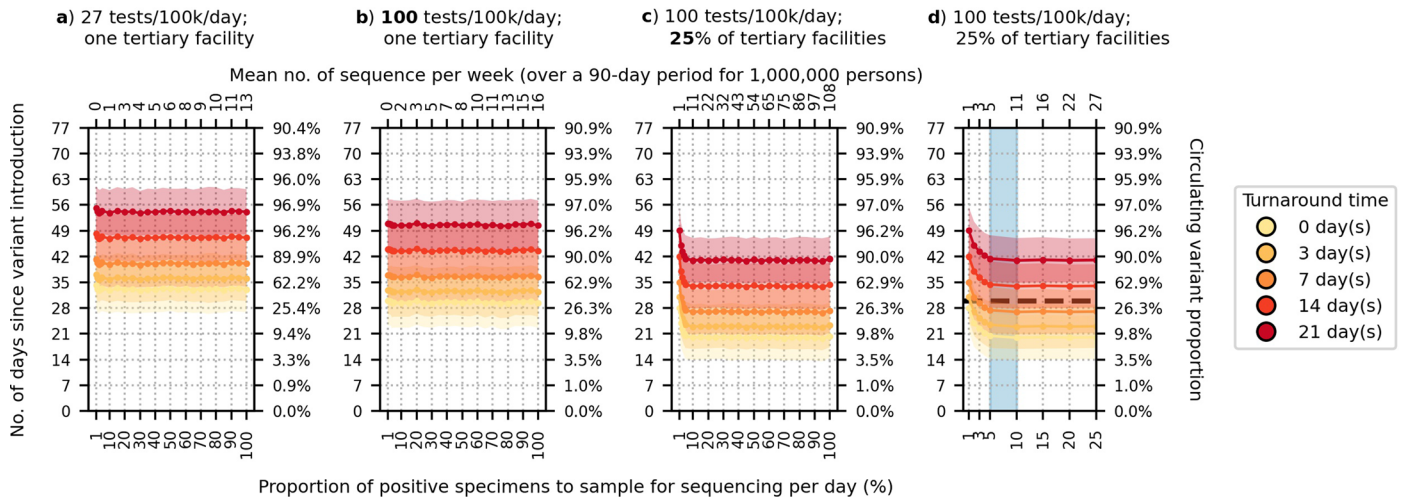
Extended Data Fig. 4 | Sensitivity analyses on accuracy of observed variant proportions for different relative transmissibility factor. Omicron-like virus properties assumed for variant and initial proportion of population with some degree of protection against the variant virus assumed at 40%. All specimens collected from the population from all healthcare facilities were sent to one facility to be sampled for sequencing (population-wide genomic surveillance

strategy). Different transmissibility factor of Omicron relative to Delta (f_{mutant}) were assumed. **(A)** Maximum absolute difference between observed and circulating variant proportions. **(B)** Proportion of timepoints when sequencing was performed that the absolute difference between observed and circulating variant proportions is greater than 20%. All results were computed from 1,000 random independent simulations for each surveillance strategy.



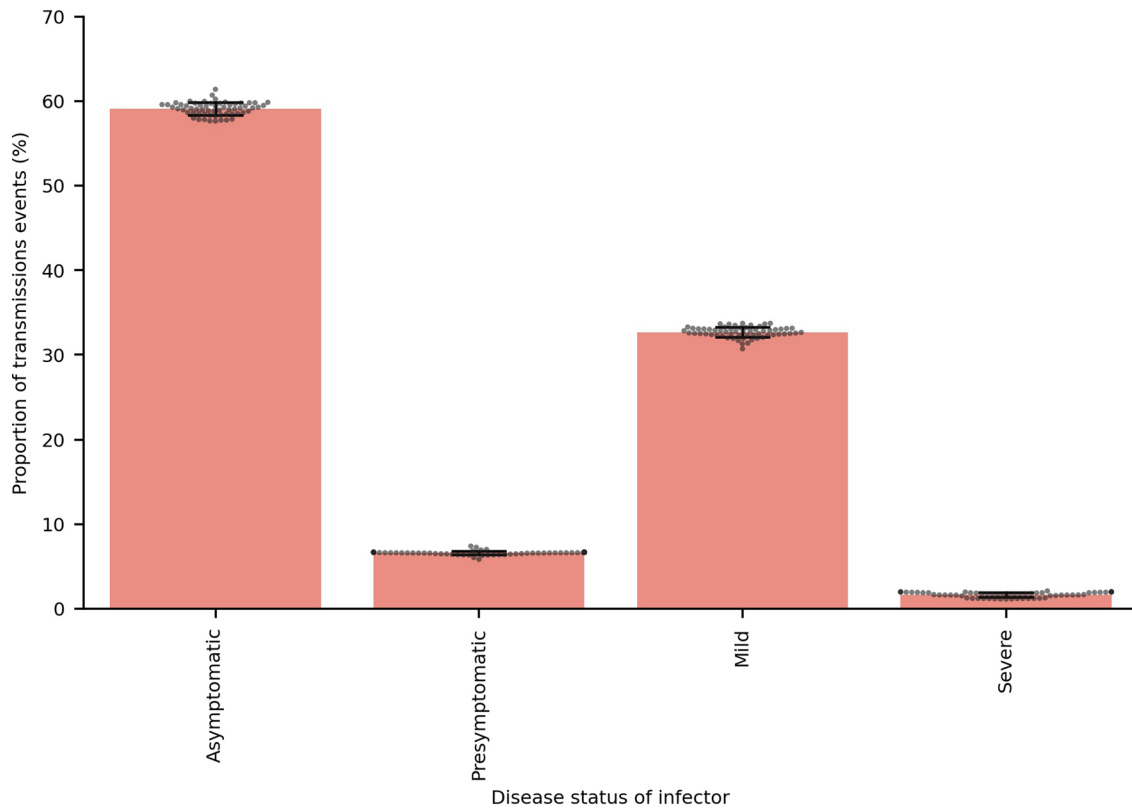
Extended Data Fig. 5 | Impact of prevalence of extant variant of concern ($I_{0,WT}$) at the time of new variant introduction. For each Ag-RDT availability (differently colored), the expected day (points and line) and the standard deviation (shaded region) when the first Omicron variant specimen (in the background of Delta) is sampled for sequencing since its introduction is plotted

against the proportion of positive specimens to be sampled for sequencing daily. Each panel shows a different prevalence of the Delta variant ($I_{0,WT}$) at the point of Omicron introduction. Sampling for sequencing was drawn from the population-wide scenario. The plotted results were computed from 1,000 random independent simulations for each surveillance strategy.

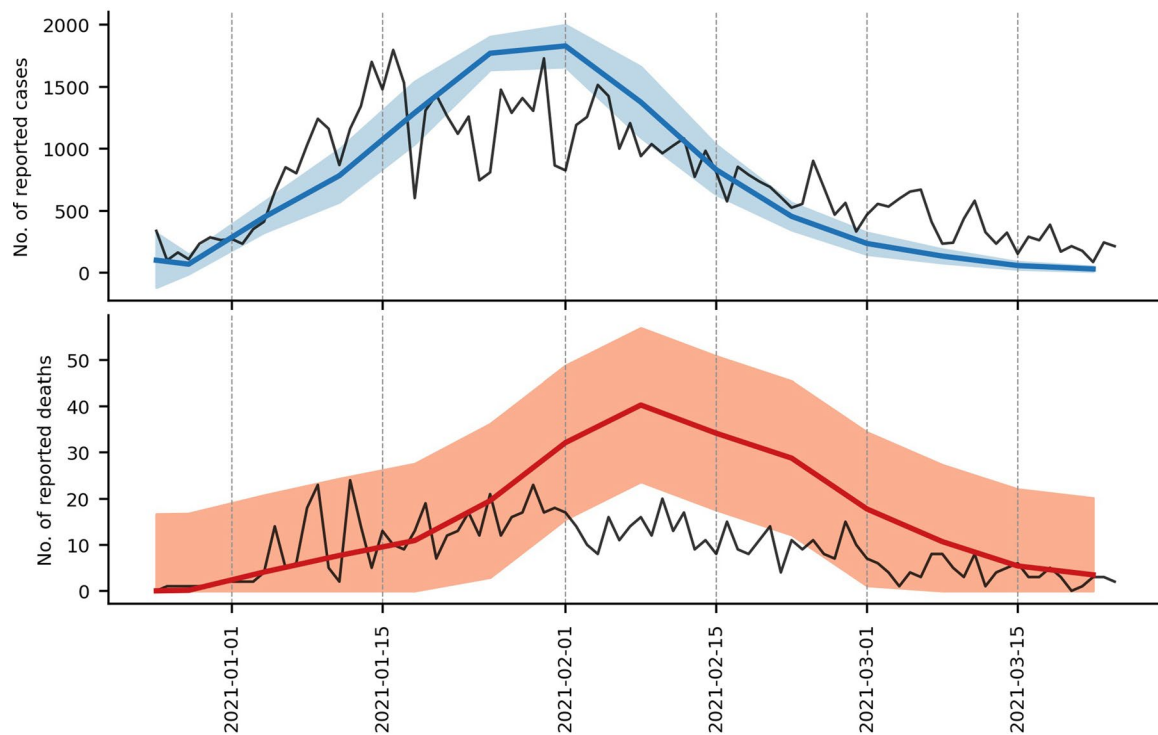


Extended Data Fig. 6 | Recommended approach to enhance genomic surveillance robustness. In each plot, the operating curves of the expected day when the first Omicron BA.1 variant sequence is generated are plotted for different proportion of specimens to sample for sequencing per day and turnaround times. We assumed that the Omicron BA.1 variant was circulating at 1% initially with Delta variant in the background. We also assumed that positive specimens sampled within each week for sequencing are consolidated into a batch before they are referred for sequencing. Turnaround time refers to the time between collection of each weekly consolidated batch of positive specimens to the acquisition of its corresponding sequencing data. The vertical axes denote the number of days passed since the introduction of the Omicron variant (left) and its corresponding circulating proportion (right). The horizontal axes denote the proportion of positive specimens to sample for sequencing per day (bottom)

and the corresponding mean number of sequences to be generated per week per 1,000,000 people over a 90-day epidemic period. **(A)** Specimen pools for sequencing from *one* tertiary facility with testing rate at 27 tests per 100,000 persons per day (tests/100 k/day). **(B)** Specimen pools for sequencing from *one* tertiary sentinel facility with testing rate at 100 tests/100 k/day. **(C)** Specimen pools for sequencing from 25% of all tertiary facilities acting as sentinel sites with testing rate at 100 tests/100 k/day. **(D)** Zoomed-in plot of **(C)** for sequencing proportions varying between 1–25%. Sequencing 5–10% of positive specimens (blue shaded region) would ensure that we would expectedly detect Omicron within 30 days if turnaround time is kept within one week. All results were computed from 1,000 random independent simulations for each surveillance strategy. The shaded region depicts the standard deviation across simulations.



Extended Data Fig. 7 | Transmissions attributed to infectors of different disease status. Proportion of transmissions events (data points) attributed to different disease status of infectors across all independent epidemic simulations ($n = 280$). Bar plots show the mean proportion with error bars denoting \pm standard deviation.



Extended Data Fig. 8 | Model validation. We compared the mean number of reported cases (blue line, top panel) and deaths (red line, bottom panel) estimated by our simulations (10 simulations in total; see Supplementary Text) against the actual case and death counts (black lines) in Lusaka, Zambia during the second wave of infections between 25 December 2020 and 24 March

2021. Actual case and death counts were retrieved from the Zambia COVID-19 Dashboard (<https://www.arcgis.com/apps/dashboards/3b3a01c1d8444932ba075fb44b119b63>). The blue and red shaded regions in each plot denotes the standard deviation of reported cases (top panel) and deaths (bottom panel) respectively.

Reporting Summary

Nature Portfolio wishes to improve the reproducibility of the work that we publish. This form provides structure for consistency and transparency in reporting. For further information on Nature Portfolio policies, see our [Editorial Policies](#) and the [Editorial Policy Checklist](#).

Statistics

For all statistical analyses, confirm that the following items are present in the figure legend, table legend, main text, or Methods section.

n/a Confirmed

- The exact sample size (n) for each experimental group/condition, given as a discrete number and unit of measurement
- A statement on whether measurements were taken from distinct samples or whether the same sample was measured repeatedly
- The statistical test(s) used AND whether they are one- or two-sided
Only common tests should be described solely by name; describe more complex techniques in the Methods section.
- A description of all covariates tested
- A description of any assumptions or corrections, such as tests of normality and adjustment for multiple comparisons
- A full description of the statistical parameters including central tendency (e.g. means) or other basic estimates (e.g. regression coefficient) AND variation (e.g. standard deviation) or associated estimates of uncertainty (e.g. confidence intervals)
- For null hypothesis testing, the test statistic (e.g. F , t , r) with confidence intervals, effect sizes, degrees of freedom and P value noted
Give P values as exact values whenever suitable.
- For Bayesian analysis, information on the choice of priors and Markov chain Monte Carlo settings
- For hierarchical and complex designs, identification of the appropriate level for tests and full reporting of outcomes
- Estimates of effect sizes (e.g. Cohen's d , Pearson's r), indicating how they were calculated

Our web collection on [statistics for biologists](#) contains articles on many of the points above.

Software and code

Policy information about [availability of computer code](#)

Data collection

Data analysis

For manuscripts utilizing custom algorithms or software that are central to the research but not yet described in published literature, software must be made available to editors and reviewers. We strongly encourage code deposition in a community repository (e.g. GitHub). See the Nature Portfolio [guidelines for submitting code & software](#) for further information.

Data

Policy information about [availability of data](#)

All manuscripts must include a [data availability statement](#). This statement should provide the following information, where applicable:

- Accession codes, unique identifiers, or web links for publicly available datasets
- A description of any restrictions on data availability
- For clinical datasets or third party data, please ensure that the statement adheres to our [policy](#)

Data on global testing rates were downloaded from <https://www.findex.org/covid-19/test-tracker>. All data used to parameterize the PATAT simulation model can be found in the Article and Supplementary Information. All simulation data generated for this study can be found in the GitHub repository (<https://github.com/AMC-LAEB/PATAT-sim>).

Human research participants

Policy information about [studies involving human research participants and Sex and Gender in Research](#).

Reporting on sex and gender	<input checked="" type="checkbox"/> This study does not involve any human research participants.
Population characteristics	<input checked="" type="checkbox"/> This study does not involve any human research participants.
Recruitment	<input checked="" type="checkbox"/> This study does not involve any human research participants.
Ethics oversight	<input checked="" type="checkbox"/> This study does not involve any human research participants.

Note that full information on the approval of the study protocol must also be provided in the manuscript.

Field-specific reporting

Please select the one below that is the best fit for your research. If you are not sure, read the appropriate sections before making your selection.

Life sciences Behavioural & social sciences Ecological, evolutionary & environmental sciences

For a reference copy of the document with all sections, see [nature.com/documents/nr-reporting-summary-flat.pdf](https://www.nature.com/documents/nr-reporting-summary-flat.pdf)

Life sciences study design

All studies must disclose on these points even when the disclosure is negative.

Sample size	No sample size calculation was performed. This is an agent-based modeling study where we simulated SARS-CoV-2 epidemics in a population of 1,000,000 individuals to study how different clinical testing and genomic surveillance strategies impact the detection of novel variants. This population size was chosen as it is sufficiently large enough to generate the desired epidemic characteristics and inferences on surveillance outcomes using reasonable amount of computing resources and computation time. We validated our simulation results based on this population size against real-life reported case data in Lusaka, Zambia (see Model Validation in Supplementary Information).
Data exclusions	N/A. Only simulation data generated from our agent-based model is used in this study and none of them was excluded from our study.
Replication	We performed 10 independent epidemic simulations for each unique parameter set (i.e. type of co-circulating variants, level of preexisting immunity in the population, testing rate). For each genomic surveillance sampling and sequencing proportion strategy applied to each epidemic simulation, we performed 100 independent simulations. For each unique epidemic and genomic surveillance parameter set, we were able to obtain a well-characterized distribution of results as described in the manuscript.
Randomization	N/A. This is a descriptive study.
Blinding	N/A. This is descriptive study.

Reporting for specific materials, systems and methods

We require information from authors about some types of materials, experimental systems and methods used in many studies. Here, indicate whether each material, system or method listed is relevant to your study. If you are not sure if a list item applies to your research, read the appropriate section before selecting a response.

Materials & experimental systems

n/a	Involvement in the study
<input checked="" type="checkbox"/>	<input type="checkbox"/> Antibodies
<input checked="" type="checkbox"/>	<input type="checkbox"/> Eukaryotic cell lines
<input checked="" type="checkbox"/>	<input type="checkbox"/> Palaeontology and archaeology
<input checked="" type="checkbox"/>	<input type="checkbox"/> Animals and other organisms
<input checked="" type="checkbox"/>	<input type="checkbox"/> Clinical data
<input checked="" type="checkbox"/>	<input type="checkbox"/> Dual use research of concern

Methods

n/a	Involvement in the study
<input checked="" type="checkbox"/>	<input type="checkbox"/> ChIP-seq
<input checked="" type="checkbox"/>	<input type="checkbox"/> Flow cytometry
<input checked="" type="checkbox"/>	<input type="checkbox"/> MRI-based neuroimaging